Available online at www.sciencedirect.com

SciVerse ScienceDirect

Ceramics International 38 (2012) 2011–2019

CERAMICS INTERNATIONAL

www.elsevier.com/locate/ceramint

Nano- and micrometre additions of SiO_2, ZrO_2 and TiO_2 in fine grained alumina refractory ceramics for improved thermal shock performance

Steffen Dudczig [a,*], Dániel Veres [a], Christos G. Aneziris [a], Erik Skiera [b], Rolf W. Steinbrech [b]

[a] Institute of Ceramic, Glass and Construction Materials, Technical University TU Bergakademie Freiberg, Freiberg 09596, Germany
[b] Institute of Energy and Climate Research, Forschungszentrum Jülich, Jülich 52425, Germany

Received 30 June 2011; received in revised form 10 October 2011; accepted 12 October 2011
Available online 18 October 2011

Abstract

The present contribution investigates the influence of micro-metre- as well as nano-metre-additions of zirconia (ZrO_2), titania (TiO_2), silica (SiO_2) and magnesia (MgO) into alumina-rich fine grained ceramic materials for refractory applications. Slip casted samples in the system alumina–zirconia–titania (AZT), alumina–zirconia–titania–silica (AZTS) and alumina–zirconia–titania–magnesia (AZTM) were sintered and the physical as well as mechanical properties were investigated as fired and after thermal shock treatments. The generation of a micro-crack network after sintering due to the formation of phases with different thermal expansion coefficients and the formation and decomposition of aluminium titanate (Al_2TiO_5) before and after thermal shock exposure leads to higher strengths after thermal shock attack.

Keywords: C. Thermal shock resistance; D. Al_2O_3; D. TiO_2; D. ZrO_2; E. Refractories

1. Introduction

The thermal shock behaviour and the spalling resistance of refractory ceramics are of a great importance during processes in the advanced secondary metallurgy and continuous metal casting not only from the point of possible failure of steel making aggregates, but also under steel quality considerations due to refractory impurities [1]. Alumina rich materials are established refractories with high refractoriness under load as well as excellent corrosion resistance in steel/slag environments. In spite these positive properties, due to their unsatisfactory thermal shock performance they are commonly used in combination with carbon for functional components such as submerged entry nozzles, slide gates, etc. [2]. The common basic principle and motivation to investigate the Al_2O_3–TiO_2–ZrO_2-system, is the formation of a micro-crack network and its contribution to tailored thermal expansion behaviour and thermal shock performance to develop carbon free high thermal shock resistant alumina-based refractory materials [3–5].

The pseudo ternary system Al_2O_3–TiO_2–ZrO_2 exhibits two basic compounds, namely aluminium titanate (Al_2TiO_5) and zirconium titanate [6]. The stoichiometric composition of zirconium titanate ranges from $ZrTiO_4$ over Zr_5TiO_{24} up to $ZrTiO_6$ (mineral: Srilankite), that means a ratio ZrO_2:TiO_2 from 1:1 to 1:2. Complete solid solubility between the first two compounds appears [7,8]. The second named compound aluminium titanate exists only in the form of Al_2TiO_5. Aluminium titanate offers the highest R_1 thermal shock parameter according to Hasselman among all other ceramic materials [9]. Al_2TiO_5 ceramics have a very low thermal expansion and a micro-crack network in the grains and at the grain boundaries induced by the high anisotropy of thermal expansion along its three crystallographic axes [10]. However, pure Al_2TiO_5 tends to decompose into Al_2O_3 and TiO_2 at temperatures ranging from 800 °C to 1300 °C during cooling as a result of eutectic reactions [11].

High-temperature neutron diffraction and differential thermal analysis have shown that the process of decomposition in metastable Al_2TiO_5 is reversible and that reformation can occur readily when decomposed Al_2TiO_5 is re-heated above 1300 °C [12]. In the same contribution it is further described that decomposition of Al_2TiO_5 during cooling below 1200 °C is controlled by temperature-dependent atomic diffusion.

* Corresponding author. Tel.: +49 3731 39 3861; fax: +49 3731 39 2419.
E-mail address: steffen.dudczig@ikgb.tu-freiberg.de (S. Dudczig).

0272-8842/$36.00
doi:10.1016/j.ceramint.2011.10.036

Following decomposition, the material does not longer exhibits a low thermal expansion coefficient or favourable thermal shock behaviour [13]. The stability of Al_2TiO_5 during heating and cooling in the range 800 °C and 1300 °C can be improved by the formation of solid solutions with MgO, Fe_2O_3 or TiO_2 which are isomorphous with the mineral pseudobrookite [14]. Another possibility of stabilization is the reduction of micro-cracks, micro-cracks growth as well as grain growth inside the Al_2TiO_5 material by the addition of additives such as silicon dioxide, zirconia, zirconium titanate or mullite. Most of them do not form a solid solution with Al_2TiO_5 as mentioned before but rather inhibit the decomposition tendency of Al_2TiO_5 [15].

The formation of either zirconium titanate or aluminium titanate in mixtures of the system Al_2O_3–TiO_2–ZrO_2 depends on the sintering temperature. Bonhomme-Coury et al. [16] demonstrated that up to a temperature of 1500 °C only zirconium titanate formation occurs. Wohlfromm et al. [17] stated that a minimum temperature of 1450 °C required for the decomposition of transitory $ZrTiO_4$ in the presence of Al_2O_3. Sintering of Al_2TiO_5–$ZrTiO_4$ composites at higher temperatures leads to a two phase microstructure, i.e. both components coexist [18]. These composite materials with high temperature stability and low thermal coefficients can be produced due to partial in situ reactions [19].

TiO_2 shows a high diffusion rate above 1000 °C [20]. The solubility of TiO_2 in Al_2O_3 is reported to vary from 800 ppm to 0.27 wt.% at temperatures between 1250 °C and 1700 °C [21]. Titania promotes the grain growth and enhances the densification of Al_2O_3 attributed to the formation of aluminium vacancies to maintain the charge neutrality [22–25]. The solubility of TiO_2 in ZrO_2 (tetragonal) varies from 13.8 mol.% at 1300 °C and 16.1 mol.% at 1500 °C [26]. The addition of TiO_2 to ZrO_2 suppresses the densification and acts as a grain growth enhancer during sintering [27].

The first eutectic melting point with increasing temperature in the system Al_2O_3–TiO_2–ZrO_2 occurs at a composition of about 60 wt.% TiO_2 and 20 wt.% Al_2O_3 and 20 wt.% ZrO_2 with a liquidus temperature of 1580 °C [28]. If MgO and other impurities like SiO_2 are present, liquid phases appear below 1400 °C [29]. An interesting approach to study the thermal expansion behaviour of ceramic composites in the system Al_2O_3–ZrO_2–TiO_2 has been presented by Virro-Nic and Pilling [30]. Compositions were prepared from mixtures of oxide powders which were compacted into cylindrical rods and then melted in a tungsten arc-image furnace. They demonstrated that compositions of 20 mol.% Al_2O_3, 20 mol.% ZrO_2 and 60% TiO_2 present a thermal expansion coefficient of -4.18×10^{-6}/K. A composition based on 40 mol.% TiO_2, 40 mol.% ZrO_2 and 20 mol.% Al_2O_3 reaches a thermal expansion coefficient of 0.5×10^{-6}/K, whereby 100 mol.% Al_2O_3 presents a thermal expansion coefficient of 8.6×10^{-6}/K, 100 mol.% $ZrTiO_4$ of 7.3×10^{-6} and 100 mol.% Al_2TiO_5 of -3.5×10^{-6}/K.

In a previous work high thermal shock resistant honeycomb structures based on a doped porous alumina matrix have been described [31]. The additions of TiO_2 and Mg-PSZ to the alumina led to higher shrinkages but also contributed to grain growth in comparison to pure alumina ceramics. Besides Al_2O_3 grains three additional zones were identified on the alumina grain boundaries. According to EDX-Analysis zone 1 was a ZrO_2-rich area with less than 0.5 wt.% MgO stabilizing agent, zone 2 a TiO_2-rich area and zone 3 a ZrO_2–TiO_2–Al_2O_3-rich area. According to a model approach dealing with the thermal expansion coefficients of the different zones, zone 1 possesses a positive thermal expansion coefficient and tries to expand during heating up and zone 2 suppress zone 1 because of its negative thermal expansion coefficient. Micro-crack rich zones are created in the composite alumina matrix that contributes to improved thermal shock performance. The ZrO_2–TiO_2–Al_2O_3-rich area (zone 3) seems to be a recrystallized melt and contributes as interconnecting phase between the Al_2O_3 grains and leads to a high coherence of the structure.

Another previous work investigated the thermal shock performance of fine grained dense slip casted materials in the system AZT. The materials with a composition of 95 wt.% Al_2O_3, 2.5 wt.% ZrO_2 (with 3.4 wt.% MgO) and 2.5 wt.% TiO_2 generate different microstructures with different phase morphologies as a function of the sintering temperature. Sintered samples at 1650 °C present relatively low starting CMOR (cold modulus of rupture) but a remarkable increase of 50% of the CMOR after quenching the samples from 1200 °C to room temperature in water. The partial decomposition of aluminium titanate into the components TiO_2 and Al_2O_3 accompanied by a shrinkage volume change has been attributed to the strengthening effect due to the generation of areas with compression stresses [32].

Investigations dealing with the thermal shock performance of magnesia partially stabilized zirconia (Mg-PSZ) with Al_2O_3- and TiO_2-additions propose two main mechanisms responsible for an enhanced thermal behaviour of composite materials in the system Al_2O_3–MgO–TiO_2–ZrO_2. Micro-crack generation caused by destabilization of the tetragonal ZrO_2 due to in situ magnesia aluminate spinel formation as well as the formation of a duplex microstructure within the Mg-PSZ-matrix. The TiO_2 addition enhances the sinter kinetics of the ZrO_2-rich system remarkably [32].

By the extension of the Al_2O_3–TiO_2–ZrO_2-system with SiO_2-additions the quaternary system Al_2O_3–TiO_2–ZrO_2–SiO_2 has to be taken under consideration. Except aluminium titanate and zirconium titanate formation $ZrSiO_4$ (zircon) and $Al_6Si_2O_{13}$ (mullite) have to be regarded. By reactive sintering of zircon/alumina/titania mixtures very dense zirconia-toughened ceramics with mullite matrix have been obtained in the temperature range between 1450 °C and 1550 °C. TiO_2 forms solid solutions with ZrO_2 and mullite with a solubility of about 4 wt.%. During the sintering process a transitory liquid phase was observed [33]. These transitory liquid phase and the formation of solid solutions controls the microstructural evolution of composite ceramics in the system Al_2O_3–TiO_2–ZrO_2–SiO_2 during sintering, as well as in post-firing heat treatments [34]. The investigation of ageing effects of zircon–alumina ceramics with small amounts of TiO_2 show after sintering that with contents above the solubility of TiO_2 in the zirconia–mullite matrix the temperature-dependent formation

or decomposition of Al_2TiO_5 plays a significant role in the long-term stability of the composite material [35].

The use of nano-metre oxides as additions to raw material mixtures or as nano-metre starting material for the production of ceramic materials is reported in a wide range of literature since several years [36–40]. Nano-metre materials are very reactive due to their high specific surface area and therefore the sintering starts at lower temperatures. Nano-metre alumina added to alumina-based ceramic raw materials can act as binder and in the sintering process the densification can be accelerated [37]. Grain-growth in ceramic materials during the sintering process can be a great problem in terms of mechanical properties. Imagawa et al. [38] reported that in mixtures of coprecipitated nano-metre ZrO_2–TiO_2 primary particles in a nano-metre Al_2O_3-matrix smaller particle sizes of ZrO_2–TiO_2 were observed after sintering in comparison to mechanical homogenised mixtures of Al_2O_3, ZrO_2 and TiO_2. The aggregation of the ZrO_2–TiO_2 primary particles during sintering could be inhibited due to the better homogenisation of the nano-metre oxide components. The addition of nano-metre particles can improve the homogeneity of dispersion ceramics. In case of a suitable dispersion step, without separation or agglomeration of the nano-metre particles, a better distribution of the added particle or reaction product of the nano-metre particles itself or with other components after sintering can be realized in a ceramic material [39].

Nano-metre oxide additions are also of great interest for unshaped refractories. Refractory castables especially self-flowing castables are characterised by their consistency after mixing, the workability, which allows them to flow and de-air easily to form a homogeneous dense structure. It is recognized that the particle size distribution of the castable is an important factor in improving the workability of the castable mixture with a low water demand. Investigations on carbon-free self-flowing castables based on alumina–magnesia spinel with additions of nano-metre oxide water-based dispersions have shown that the flowability can be improved significantly. The properties of the added dispersion must be adjusted to the properties of the castable, especially the pH-value and the isoelectric point (IEP) [40].

In the present work the influence of zirconia (ZrO_2), titania (TiO_2), silica (SiO_2) and magnesia (MgO) additions to alumina-rich refractory materials is investigated. Furthermore the influence of the grain size of the additions (micro-metre or nano-metre) on the material properties is discussed before and after thermal shock treatment.

Table 1
Commercial available nano-metre particle dispersions with their own temporary additives.

Product	VPDisp W2650x	VPDisp W740x	VPDisp W7330
Oxide	ZrO_2	TiO_2	SiO_2
Water (wt.%)	50	60	70

2. Materials and methods

The used raw materials the system A–Z–T were alumina Martoxid MR70 (Martinswerk, Germany) with a d_{50} of 0.8 μm, partially stabilized zirconia with 3.4 wt.% MgO as stabilizing agent (Unitec, USA) with a d_{50} of 1.3 μm and titania T-R (Crenox, Germany) with a d_{50} of 1.0 μm. For preparing AZTS-samples, fused silica AMOSIL 510 (Quarzwerke Frechen, Germany) with a d_{50} of 11 μm was used. To investigate the influence of particle size of TiO_2, ZrO_2 and SiO_2 water-based nano-metre dispersions (Evonik, Germany), listed in Table 1, were used for preparing the AZTn- and AZTSn-samples. The water content of the dispersions was deducted from the used water content for the slurry.

For a possible stabilization of Al_2TiO_5 in the AZT composition, 1.0 wt.% magnesium oxide was added in form of 1.45 wt.% magnesium hydroxide $Mg(OH)_2$ (Merck, Germany) to bypass delayed hydration effects. These are caused by the reaction of MgO with water to form Brucite $Mg(OH)_2$ accompanied by a volume expansion more than 50 vol.%.

Samples have been prepared using slip casting technology and the compositions are listed in Table 2. The raw materials were mixed with de-ionized water with a weight ratio powder/water of 75/25. Organic additives were 0.3 wt.% Dispex A40 (Ciba, Germany) and 0.15 wt.% Optapix AC170 (Zschimmer & Schwarz, Germany) related to the solids. The components were mixed and homogenised in a polyethylene chamber with alumina milling media for five hours. The prepared slip was casted in plaster moulds of 3 mm × 4 mm × 45 mm sample dimensions, demoulded after 5 h and dried at 120 °C. The

Table 2
Compositions of the investigated samples in wt.%.

Component	Product	Samples				
		AZT	AZTn	AZTS	AZTSn	AZTM
Al_2O_3	Martoxid MR 70	95.0	95.0	90.0	90.0	93.55
ZrO_2	P59	2.5		2.5		2.5
Nano-ZrO_2	VPDisp W2650x		2.5[a]		2.5[a]	
TiO_2	T-R	2.5		2.5		2.5
Nano-TiO_2	VPDisp W740x		2.5[a]		2.5[a]	
SiO_2	AMOSIL 510			5.0		
Nano-SiO_2	VPDisp W7330				5.0[a]	
$Mg(OH)_2$						1.45

[a] Solid component of the dispersion.

samples were sintered at 1500 °C and 1650 °C respectively with a heating rate of 2 K/min and a holding time of 2 h in an electrical furnace (Nabertherm HT 21/18) in oxidizing atmosphere.

The porosity of the sintered samples was measured with the aid of mercury intrusion porosimetry (Pascal 140/440, Thermo Electron). Three point bending strengths were measured at room temperature according to DIN EN 843 after sintering as well as after thermal shock treatment in water from 1200 °C with respect to DIN 51068 for one and five cycles on as sintered samples.

Phase compositions were determined using X-ray diffraction analysis (XRD) with the aid of a Philips diffractometer and analysed with PANalytical X'PERT HighScore Plus. For the XRD measurements the samples were grinded in a vibratory mill and sieved via a 63 μm mesh. Microstructural characterisation was carried out using scanning electron microscopy (SEM) an energy dispersive X-ray microanalysis (EDX).

3. Results and discussion

The AZT-samples sintered at 1500 °C and at 1650 °C present an open porosity of 1.2% and 5.2% respectively (Table 3). The samples sintered at 1500 °C possess a high strength at room temperature due to the low open porosity and less grain growth as well as no micro-crack network generation. After quenching from 1200 °C in water (25 °C) a rapid loss in strength was measured, demonstrating thermal shock behaviour as discussed by Hasselman for fine grained dense alumina ceramics [41,42]. In contrast to these results, AZT-samples sintered at 1650 °C presented an unexpected mechanical performance. After sintering at 1650 °C the AZT-samples achieved very low strengths, mainly due to the grain growth of the fine alumina (compare Figs. 1 and 2) and due to a micro crack network generation. In contrast to the expected thermal shock behaviour of fine grained alumina ceramics the AZT-samples sintered at 1650 °C show an increase of residual strength of 90% after the 1st thermal shock and 60% after 5th thermal shock compared to the as sintered state.

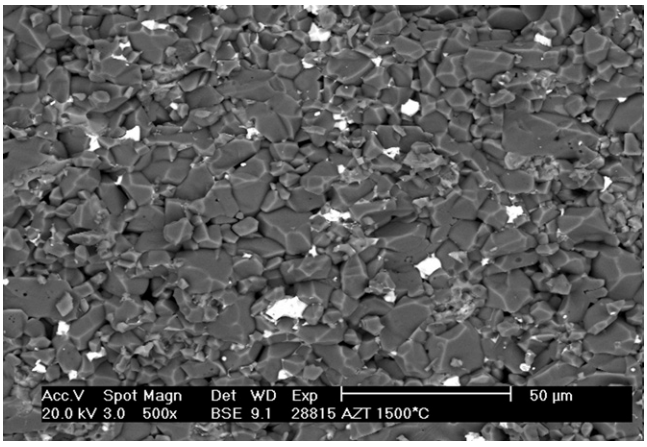

Fig. 1. SEM-micrograph of a AZT-sample sintered at 1500 °C, magnification 500×.

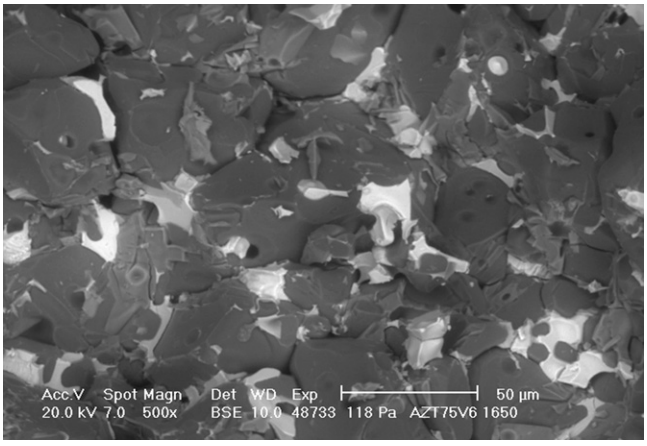

Fig. 2. SEM-micrograph of a AZT-sample sintered at 1650 °C, magnification 500×.

In order to examine the influence of the particle size for the microstructure generation, nano-metre dispersions of TiO_2 and

Table 3
Physical and mechanical properties of AZT- and AZTn-materials as sintered and after quenching from 1200 °C (standard deviation in brackets).

Treatment	Open porosity (%)	Density (g/cm^3)	CMOR (MPa)	CMOR after thermal shock (MPa)	CMOR loss after thermal shock (±%)
AZT 1500 °C	1.2	3.86	185.2 (±10.8)		
1200 °C				48.2 (±6.16)	−73.98
5× 1200 °C				24.9 (±5.47)	−86.55
AZT 1650 °C	5.18	3.86	5.22 (±0.5)		
1200 °C				9.9 (±1.71)	90.04
5× 1200 °C				8.4 (±1.70)	60.54
AZTn 1500 °C	0.84	3.95	205.0 (±19.05)	–	
1200 °C				46.0 (±8.62)	−77.56
5× 1200 °C				28.9 (±5.68)	−85.88
AZTn 1650 °C	5.09	3.8	7.9 (±0.38)	–	–
1200 °C				11.8 (±0.69)	47.8
5× 1200 °C				11.4 (±1.84)	43.9

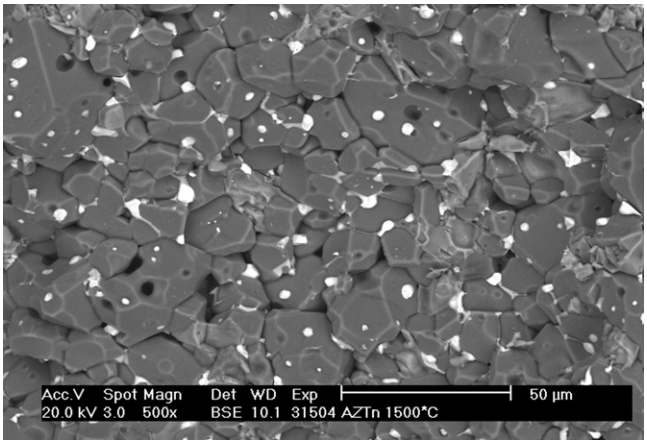

Fig. 3. SEM-micrograph of a AZTn-sample sintered at 1500 °C, magnification 500×.

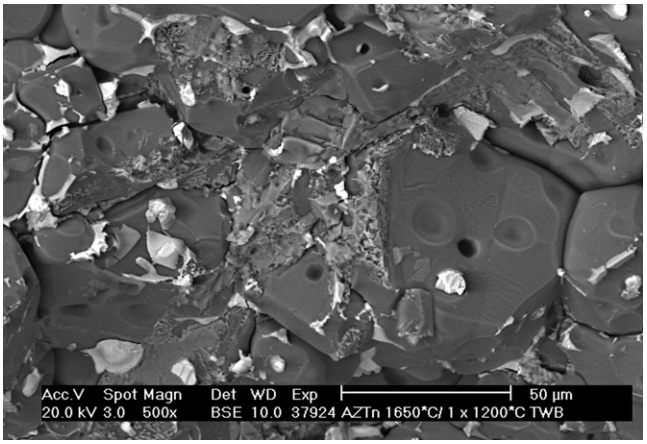

Fig. 5. SEM-micrograph of a AZTn-sample sintered at 1650 °C, after thermal shock from 1200 °C, magnification 500×.

ZrO_2 were added to the alumina matrix. It can be assumed that well pre-dispersed nano-particles led to a better distribution of the dispersing phase. For the AZTn-samples sintered at 1500 °C and 1650 °C an open porosity of 0.84% and 0.51% respectively was determined. Furthermore an increase in cold modulus of rupture of 10% (1500 °C) and 50% (1650 °C) could be registered. After the 1st thermal shock, the AZTn-samples sintered at 1500 °C lost their strength rapidly, as already observed for the AZT-composition sintered at the same temperature. On the other hand, the AZTn-samples sintered at 1650 °C showed an increase of the residual strength of 48% after the 1st and 44% after the 5th thermal shock compared to the as-sintered state. In comparison to AZT-samples the AZTn-compositions achieved approximately half of the strength increase after the 1st thermal shock. The lower strength increase of the AZTn-samples after the 1st thermal shock could be contributed to less decomposition of the aluminium titanate phase derived from the finer crystalline structure that was generated by the using nano-particles. A higher destabilization rate can be observed with increasing grain size of the alumina titanate micro structures in comparison to fine aluminium titanate structures as investigated in Cleveland and Bradt [43].

Figs. 1–4 display typical SEM-micrographs of AZT- and AZTn-samples sintered at 1500 °C and 1650 °C respectively. The influence of the sintering temperature on the grain growth of the alumina grains is clearly visible. The AZT-zone 3 that was already registered in a previous work [31] can also be identified for the samples sintered at 1650 °C and is better distributed using nano-metre additions. In both compositions, AZT and AZTn, sintered at 1650 °C additional zirconia and aluminium titanate phases have been identified at the grain boundaries. After thermal shock from 1200 °C, rutile crystals from the decomposition of the aluminium titanate at the alumina grain boundaries have been identified (Figs. 5 and 6). Thereby at the AZTn-samples less rutile can be identified after quenching. This is probably related to the lower decomposition rate of the aluminium titanate phase that leads also to lower residual strength increase of the AZTn-compositions after 5 thermal shocks.

In Figs. 9 and 10 the phase composition of sintered and quenched samples after the 1st and 5th thermal shock are presented. The phases identified are Al_2TiO_5, $ZrTiO_4$, monoclinic and traces of tetragonal ZrO_2. After quenching from 1200 °C in water, a new phase composition was identified.

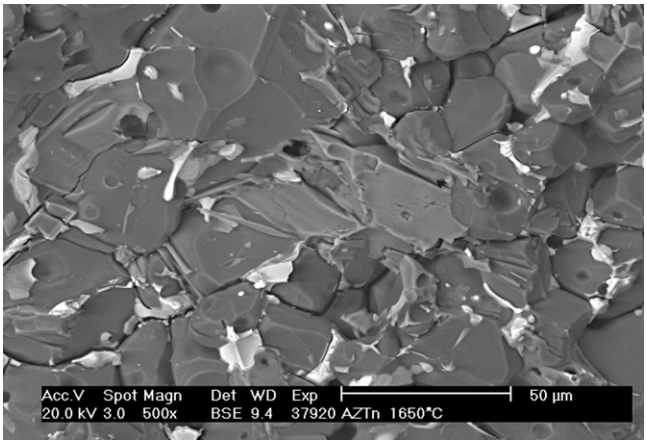

Fig. 4. SEM-micrograph of a AZTn-sample sintered at 1650 °C, magnification 500×.

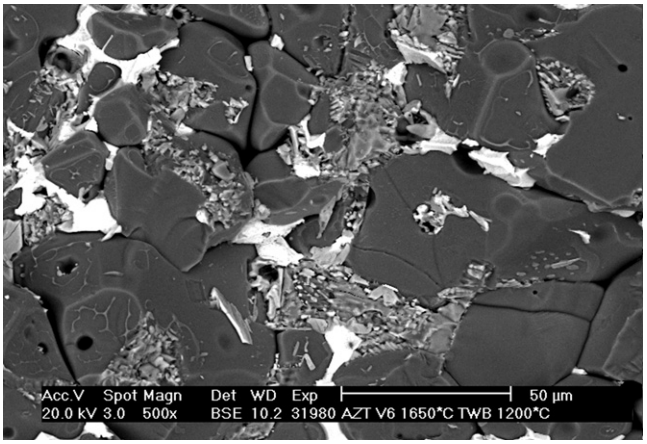

Fig. 6. SEM-micrograph of a AZT-sample sintered at 1650 °C, after thermal shock from 1200 °C, magnification 500×.

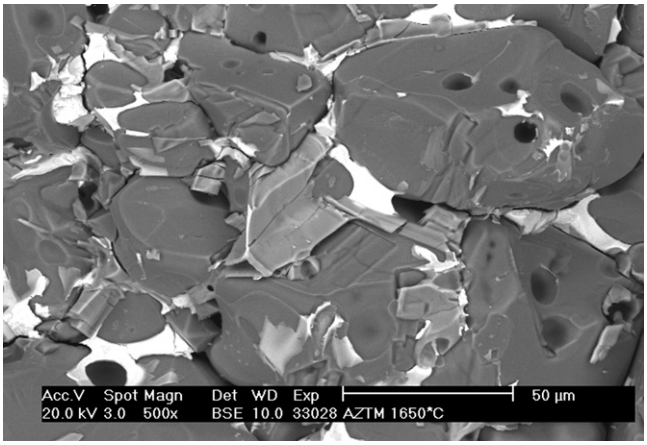

Fig. 7. SEM-micrograph of a AZTM-sample sintered at 1650 °C, magnification 500×.

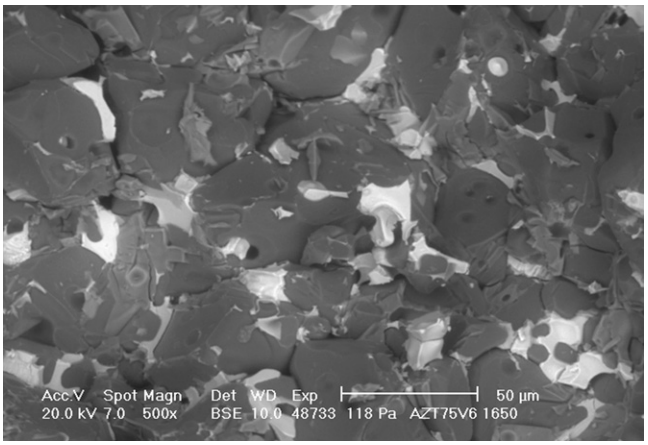

Fig. 8. SEM-micrograph of a AZT-sample sintered at 1650 °C, magnification 500×.

Independently from the sintering temperature and the starting composition, quenching led to the partial decomposition of Al_2TiO_5. After the first quenching, Al_2TiO_5-peaks at 18.8° (2 0 0) and 26.5° (101) are reduced and TiO_2-peak (rutile) at 27.4° (1 1 0) can be clearly identified. Furthermore, after 5 quenching cycles, no Al_2TiO_5 can be identified in AZT- and also in AZTn-samples sintered at 1650 °C. In sum the AZTn-samples present after sintering, as well as after the first and fifth thermal shock higher strength in compare to AZT-samples.

To prove this beneficial influence of the decomposition of the Al_2TiO_5 in the AZT-samples on the thermal shock behaviour, a composition doped with a small amount of MgO, in form of $Mg(OH)_2$, was studied (AZTM-composition). MgO is identified as a stabilizer for the Al_2TiO_5 phase [45]. As

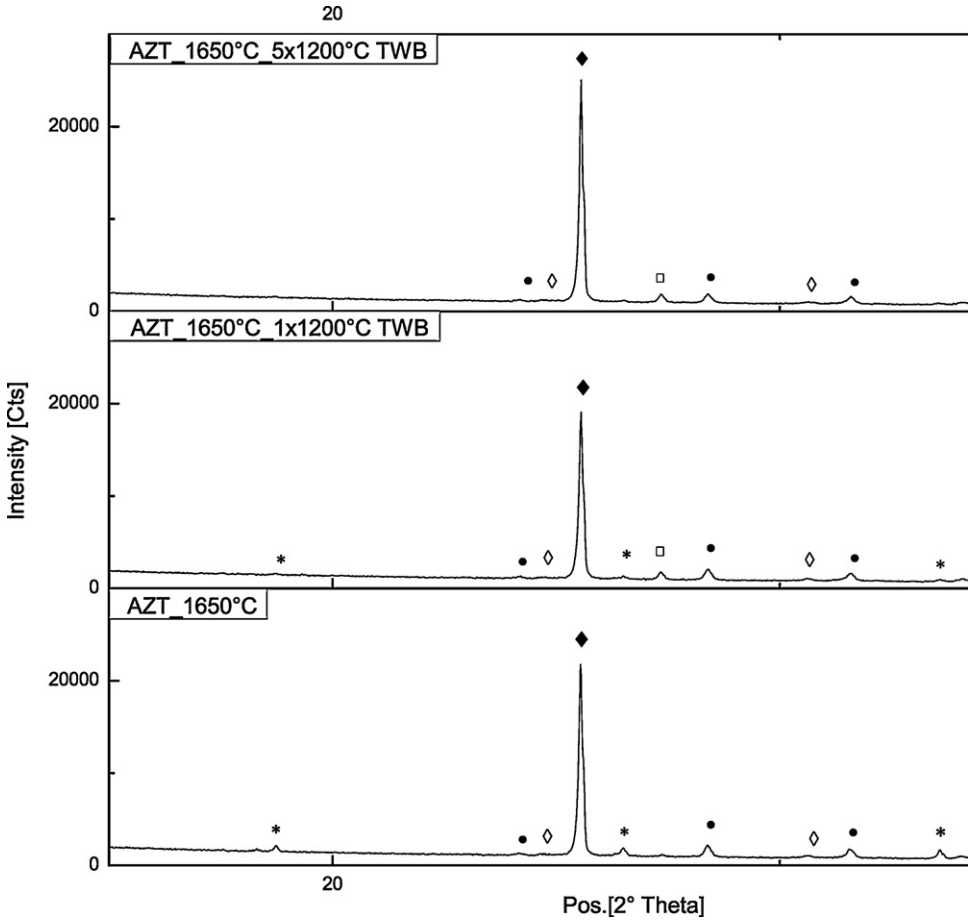

Fig. 9. XRD of AZT sintered at 1650 °C as well as after quenching from 1200 °C one and five times.

Figs. 7 and 8 show the MgO did not work as grain growth inhibiter as reported by Bae and Baik [46]. The CMOR of the AZTM-samples sintered at 1650 °C lies in the same level as the CMOR of the AZT-samples after the same thermal treatment. However, there was no increase in the residual strength after thermal shock. During the thermal shock the AZTM-samples perform the usual strength decrease as already presented in fine grained ceramics. According to the phase composition of the

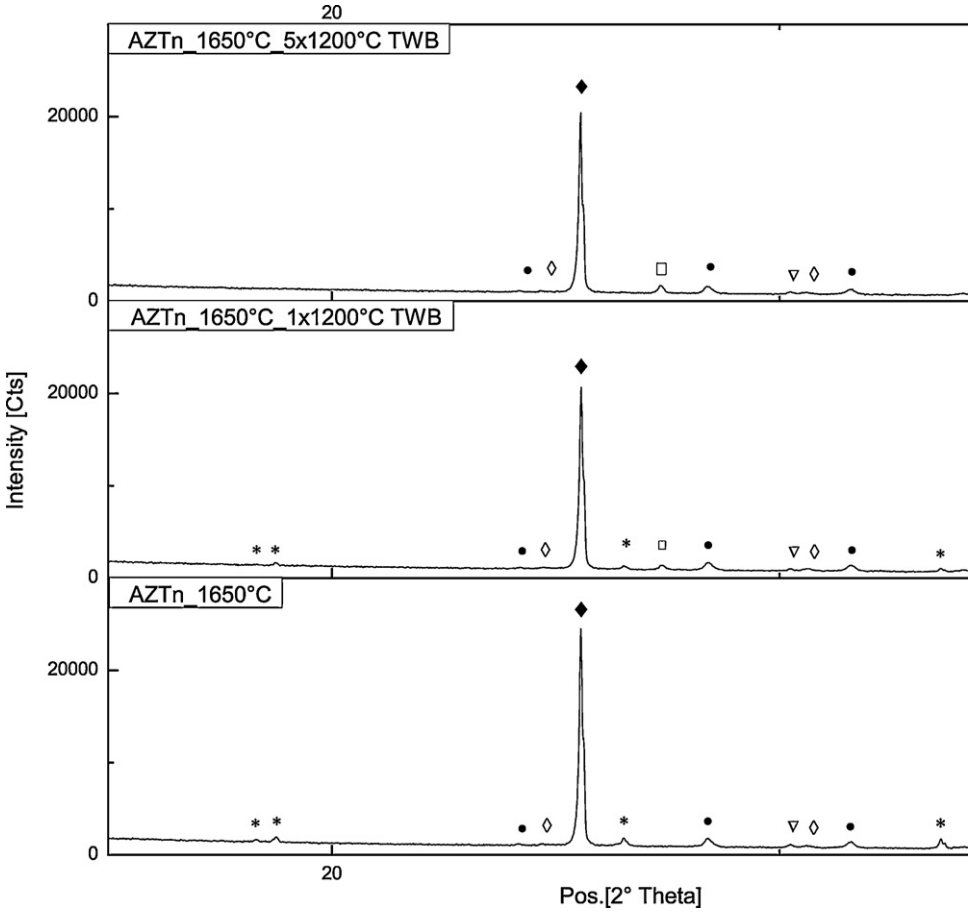

Fig. 10. XRD of AZTn sintered at 1650 °C as well as after quenching from 1200 °C one and five times.

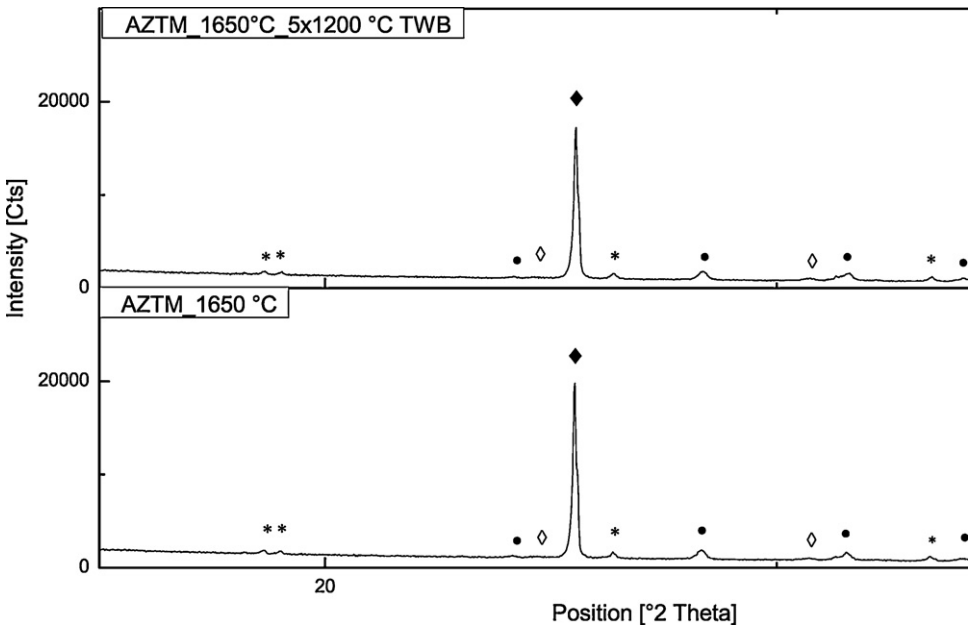

Fig. 11. XRD of AZTM sintered at 1650 °C as well as after quenching from 1200 °C five times.

Table 4
Physical and mechanical properties of AZTS- and AZTSn-materials as sintered and after quenching from 1200 °C (standard deviation in brackets).

Treatment	Open porosity (%)	Density (g/cm^3)	CMOR (MPa)	CMOR after thermal shock (MPa)	CMOR loss after thermal shock (±%)
AZTS_1500 °C	1.28	3.49	151.7 (±9.65)	–	
1200 °C				31.4 (±5.67)	−79.27
5× 1200 °C				10.4 (±2.45)	−93.17
AZTS_1650 °C	1.13	3.55	85.2 (±8.50)	–	–
1200 °C				31.6 (±3.64)	−62.92
5× 1200 °C				7.1 (±1.29)	−91.63
AZTSn_1500 °C	0.58	3.66	142.2 (±16.44)	–	
1200 °C				28.6 (±4.88)	−79.87
5× 1200 °C				11.4 (±3.53)	−91.99
AZTSn_1650 °C	1.13	3.55	101.8 (±12.23)	–	–
1200 °C				29.6 (±4.90)	−70.91
5× 1200 °C				10.1 (±2.35)	−90.06

AZTM-samples no decomposition of the aluminium titanate phase was identified (Fig. 11).

The quaternary system alumina–zirconia–titania–silica (AZTS) and alumina with nano addition of zirconia–titania–silica (AZTSn) was also studied, in order to verify the effect of the mullitization of the matrix on the thermal shock properties of the AZT-ceramic. Mullite is generally reported as phase which enhances thermal shock resistance, especially when mullite is introduced in an alumina ceramic matrix due to different thermal expansion coefficients. Compositions with both micro- and nano-SiO_2-additions were studied as listed in Table 2. The AZTS-samples presented an open porosity after sintering at 1500 °C of 1.28%. By sintering at a temperature of 1650 °C an open porosity of 1.13% was obtained (Table 4). The phase composition results are shown in Fig. 12. The strength at room temperature was lower in comparison to AZT-samples, despite the lower apparent porosity. The AZTS- and AZTSn-samples had a rapid loss in the residual strength, showing that the presence of mullite in this particularly AZT-system does not provide an improvement of the thermal shock performance.

4. Conclusions

Low porous fine grained alumina ceramics with small amounts of zirconia and titania additions were investigated. As in the previous paper [44] presented, the zirconia and titania doped alumina ceramics, sintered at 1650 °C generate composite micro structures with improved thermal shock performance. Quenching the samples from 1200 °C into water decomposition of the Al_2TiO_5 is generated accompanied by a volume shrinkage and generating areas with tensile stresses. The aluminium titanate free areas between the alumina grains causes compressive stresses, that are believed to lead to the increase of the residual strength after thermal shock.

In case of nano-metre zirconia and titania dispersions, a better homogeneous distribution of the oxide additions

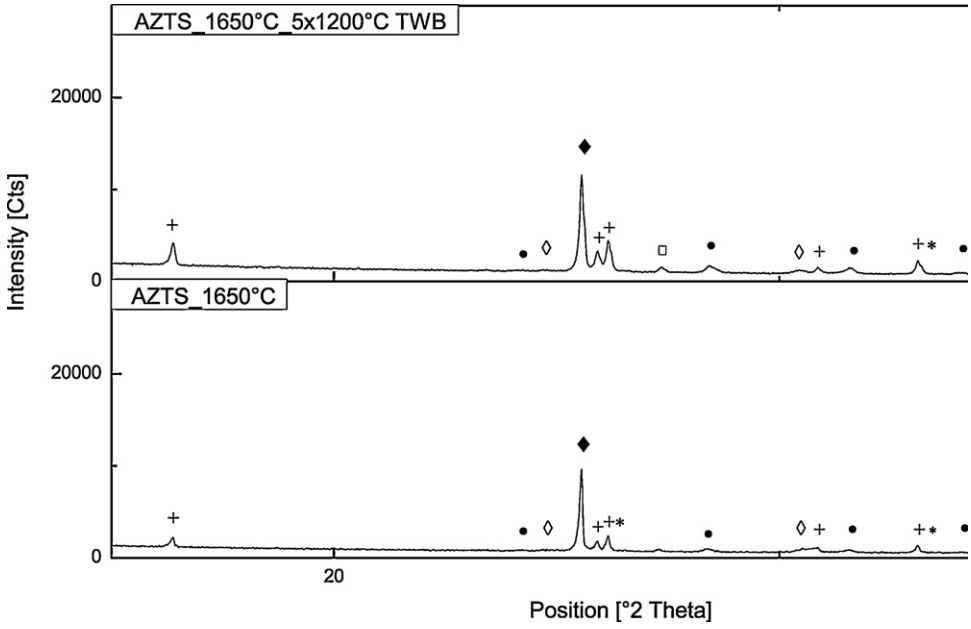

Fig. 12. XRD of AZTS sintered at 1650 °C as well as after quenching from 1200 °C five times.

in the alumina matrix has been achieved according to SEM-micrographs. In addition higher strengths have been registered at the 1650 °C sintering temperature. Due to the thermal shock treatment partial decomposition of the Al_2TiO_5 occurs followed by an increase of the residual strength. In comparison to AZT-samples a slightly lower increase of the strengths has been identified but in sum higher absolute values have been achieved after sintering, after the first and the fifth thermal shock. It is assumed that the zone 3 as already mentioned by Aneziris et al. [31] contributes to better connection between the alumina grains.

In this work the benefit of the decomposition of the Al_2TiO_5 was proved. The results of the AZTM-samples clearly showed that without the decomposition of Al_2TiO_5 no increase of the residual strength could be obtained.

Based on these results fine grained alumina functional components for the iron and steel industry – such as submerged entry nozzles – with lower or no carbon additions could be investigated in the future. Further in a future contribution the ''work of fracture'' will be measured according to Skiera et al. [47] and will be correlated to the thermal shock performance of the new developed AZT- and AZTn-compositions.

Acknowledgements

The authors would like to thank the German Scientific Foundation (DFG) for supporting the investigations in terms of the Priority Program SPP 1418 ''Refractory Initiative for the Reduction of Emissions – FIRE''. Also would like to thank Dr. Tontrupp from the company Evonik industries (Germany) for supplying the nano suspensions for the research work.

References

[1] C.G. Aneziris, U. Klippel, W. Schärfl, V. Stein, Y. Li, Int. J. Appl. Ceram. Technol. 4 (6) (2007) 481.
[2] Y. Li, C.G. Aneziris, X.X. Yi, N. Li., Refract. Manual Interceram. Int. (2005) 20.
[3] I.J. Kim, K.S. Lee, C.G. Aneziris, Key Eng. Mater. 336–338 (2007) 2448.
[4] F.J. Parker, J. Am. Ceram. Soc. 73 (1990) 929.
[5] E.H. Lutz, M.V. Swain, J. Am. Ceram. Soc. 75 (1992) 3058.
[6] Al_2O_3–TiO_2–ZrO_2-phase diagram, ACerS–NIST Phase Equilibria Diagrams, Version 3.1, 2005.
[7] U. Troitzsch, A.G. Christy, D.J. Ellis, Phys. Chem. Miner. 32 (2005) 504.
[8] C.L. Wang, H.Y. Lee, F. Azough, R. Freer, J. Mater. Sci. 32 (1997) 1693.
[9] C.G. Aneziris, E. E. Pfaff, H.R. Maier, Key Eng. Mater. 132–136 (1997) 1829.
[10] Y. Ohya, Z. Nakagawa, J. Am. Ceram. Soc. 70 (8) (1987) C184.
[11] G. Bayer, J. Less Common. Met. 24 (2) (1971) 129.
[12] I.M. Low, Z. Oo, Mater. Chem. Phys. 111 (2008) 9.
[13] V. Buscaglia, P. Nanni, J. Am. Ceram. Soc. 81 (10) (1998) 2645.
[14] I.J. Kim, H.S. Kwak, Can. Metall. Quart. 39 (4) (2000) 387.
[15] A.H. Mchale, R.S. Roth, R.S., J. Am. Ceram. Soc. 20 (1983) C-18.
[16] L. Bonhomme-Coury, N. Lequeux, S. Mussotte, J. Sol–Gel Sci. Technol. 2 (1994) 371.
[17] H. Wohlfromm, J.S. Moya, P. Pena, J. Mater. Sci. 25 (1990) 3753.
[18] C. Hyung, L. Kim, S. Kee, I.J. Kim, C.G. Aneziris, J. Eur. Ceram. Soc. 27 (2007) 1431.
[19] E. Pfaff, in: J. Kriegesmann (Ed.), Technische Keramische Werkstoffe, German Ceramic Society, 1997.
[20] R.S. Nasar, M. Cerqueira, E. Longo, J.A. Varela, Ceram. Int. 30 (2004) 571.
[21] Y.-M. Kim, S.-H. Hong, D.-Y. Kim, J. Am. Ceram. Soc. 83 (11) (2000) 2809.
[22] R.D. Bagley, I.B. Cutler, D.L. Johnson, J. Am. Ceram. Soc. 53 (3) (1970) 136.
[23] R.J. Brook, J. Am. Ceram. Soc. 55 (2) (1972) 114.
[24] K. Hamano, C.-S. Hwang, Z. Nakagawa, Y. Ohya, Yogyo Kyokaishi 94 (5) (1986) 505.
[25] T. Ikegami, K. Kotani, J. Am. Ceram. Soc. 70 (12) (1987) 885.
[26] C.L. Lin, D. Gan, P. Shen, Mater. Sci. Eng. A 129 (1990) 147.
[27] S.X. Zhang, J.B. li, J. Gao, H.Z. Zhai, B. Zhang, J. Eur. Ceram. Soc. 21 (16) (2001) 2931.
[28] P. Miranzo, P. Pena, J.S. Moya, S.D. Aza, J. Mater. Sci. 20 (1985) 2702.
[29] M.F. Melo, J.S. Moya, P. Pena, S.D. Aza, J. Mater. Sci. 20 (1985) 2711.
[30] P. Virro-Nic, J. Pilling, J. Mater. Sci. Lett. 13 (1994) 950.
[31] C.G. Aneziris, W. Schärfl, B. Ullrich, J. Eur. Ceram. Soc. 27 (2007) 3191.
[32] T. Kratschmer, C.G. Aneziris, Appl. Ceram. Technol. 8 (2) (2011) 398.
[33] M.F. Melo, J.S. Moya, P. Pena, S. D.E. Aza, J. Mater. Sci. 20 (1985) 2711.
[34] J.S. Moya, P. Miranzo, M.I. Osendi, Mater. Sci. Eng. A 109 (1989) 139.
[35] M.F. Melo, J.S. Moya, J. Mater. Sci. 25 (1990) 2082.
[36] T.V. Rymon Lipinski, C. Tontrup, UNITECR 2007, Proceedings, p. 391.
[37] H. Hahn, Adv. Eng. Mater. 5 (5) (2003) 277.
[38] H. Imagawa, T. Tanaka, N. Takahashi, S. Matsunaga, A. Suda, J. Catal. 251 (2007) 315.
[39] M.I Nieto, C. Baudín, I. Santacruz, Ceram. Int. 37 (2011) 1085.
[40] C.G. Aneziris, S. Dudczig, Adv. Sci. Technol. 70 (2010) 72.
[41] D.P.H. Hasselman, Ceram. Bull. 49 (12) (1970) 1033.
[42] D.P.H. Hasselman, J. Am. Ceram. Soc. 52 (11) (1969) 600.
[43] J.J. Cleveland, R.C. Bradt, J. Am. Ceram. Soc. 16 (11–12) (1978) 478.
[44] C.G. Aneziris, S. Dudczig, N. Gerlach, H. Bereck, D. Veres, Adv. Eng. Mater. 12 (6) (2010) 478.
[45] V. Buscaglia, P. Nanni, G. Battilana, G. Aliprandi, C. Carry, J. Eur. Ceram. Soc. 13 (1994) 411.
[46] S.I. Bae, S. Baik, J. Am. Ceram. Soc. 77 (10) (1994) 2499.
[47] E. Skiera, J. Malzbender, J. Mönch, S. Dudczig, C.G. Aneziris, Presentation MSE 2010 Congress, Darmstadt, Germany, August 24–26, 2010.